Journal of Alloys and Compounds 509 (2011) 10161–10166

Contents lists available at SciVerse ScienceDirect

Journal of Alloys and Compounds

journal homepage: www.elsevier.com/locate/jallcom

A carbon-free $LiFePO_4$ cathode material of high-rate capability prepared by a mechanical activation method

Yuehui Yin, Mingxia Gao*, Jilai Ding, Yongfeng Liu, Lukai Shen, Hongge Pan

State Key Laboratory of Silicon Materials & Department of Materials Science and Engineering, Zhejiang University, Hangzhou, 310027, PR China

ARTICLE INFO

Article history:
Received 12 June 2011
Received in revised form 13 August 2011
Accepted 16 August 2011
Available online 22 August 2011

Keywords:
Electrode materials
$LiFePO_4$
Chemical synthesis
Iron phosphides
High-rate capability

ABSTRACT

A carbon-free $LiFePO_4$ cathode material for lithium–ion battery has been synthesized by a mechanical activation method. High electron conductive iron phosphides (Fe_2P/FeP) are in situ introduced into the products during the calcination process in order to improve the high rate capability of the $LiFePO_4$ materials. The amount of the iron phosphides is adjusted by the calcination time. The study of the structure and electrochemical performance of the $LiFePO_4$ products shows that the calcination time imposes minor effect on the size and shape of the $LiFePO_4$ particles, but varies the phase structure, crystallinity and finally the electrochemical performance of the $LiFePO_4$ products as a consequence. The content of Fe_2P/FeP increases gradually with the calcination time. Suitable amount of Fe_2P/FeP and good crystallinity play effective role in improving the high-rate capability of the carbon-free $LiFePO_4$ material. Specific discharge capacities over 110 mAh/g at 5 C and 100 mAh/g at 10 C are obtained for the $LiFePO_4$ material containing 4–5 wt.% Fe_2P/FeP.

1. Introduction

Olivine $LiFePO_4$ has attracted extensive attention as one of the promising cathode materials for lithium ion rechargeable batteries since the pioneering work of Padhi et al. [1]. Due to its well-known advantages, such as the excellent thermal stability, low cost and environmental benignancy, etc., $LiFePO_4$ is expected to be applied in the high power batteries for powering electric vehicle and hybrid electric vehicle, etc. But the drawbacks of low electronic conductivity (ca. 10^{-9} S/cm) [2] and low Li ion diffusion rate within particles (ca. 10^{-16}–10^{-14} cm^2/s) [3,4] for $LiFePO_4$ undermine greatly the rate performance of the material. Therefore, intensive effort has been devoted to improve the electric conductivity of the material. Coating high conductivity phase (generally carbon) [5–8], reducing particle size [9,10] and doping with super valence ions [11–15], etc., are all effective ways in enhancing electric conductivity, consequently improve the high-rate capability of $LiFePO_4$. Moreover, in many cases, carbon coating and particles minimization to nano scale are simultaneously adopted [16,17]. Besides, it was ever reported that the introduction of Fe_2P phase in $LiFePO_4$ enhance dramatically the electronic conductivity of $LiFePO_4$ from ca. 10^{-9} to 10^{-2} S/cm [18]. The formation of Fe_2P shows metallic type conductivity on the surface of the $LiFePO_4$ grains in the course of phospho-olivine synthesis [19]. The favorable effect of Fe_2P on the kinetic electrochemical performance of $LiFePO_4$ has been recognized gradually [19–22].

Carbon coating has been proved as an effective way to improve the rate performance of $LiFePO_4$ cathode. However, Chen and Dahn [23] demonstrated that even 3 wt.% of carbon coating decreased the tap density of $LiFePO_4$ by over 40%. Therefore, carbon-free $LiFePO_4$ is expected beneficial in improving the specific volumetric capacity of $LiFePO_4$ material. Carbon-free $LiFePO_4$ materials have been reported possessing high-rate capability in previous literature, but commonly, nano-size particles [24,25] are required, which lead to a low tap density and hence decreases the specific volumetric capacity of the $LiFePO_4$ [26].

The present study intends to prepare a carbon-free $LiFePO_4$ material with moderate particle size (sub-micron). In order to improve electronic conductivity of the $LiFePO_4$ materials, high electron conductive iron phosphides (Fe_2P/FeP) are in situ introduced during the fabrication process. As the mass density of Fe_2P/FeP is more than twice higher than that of carbon, the carbon-free $LiFePO_4$ material containing Fe_2P/FeP is considered beneficial in increasing its packing density. Considering the negative effect of the carbon coating on the packing density on the cathode material, the introduction of Fe_2P/FeP rather than carbon coating is expected beneficial in improving the specific volumetric capacity of the $LiFePO_4$ cathode material. But Fe_2P is electrochemically inactive [21] and FeP should be inactive, too, and other inactive impurities such as Li_3PO_4, etc. form with the formation of the Fe_2P/FeP phases, therefore the amount of Fe_2P/FeP should be carefully optimized. In the present study, a mechanical activation method was adopted to

* Corresponding author. Tel.: +86 571 87952615; fax: +86 571 87952615.
E-mail address: gaomx@zju.edu.cn (M. Gao).

0925-8388/$ – see front matter © 2011 Elsevier B.V. All rights reserved.
doi:10.1016/j.jallcom.2011.08.067

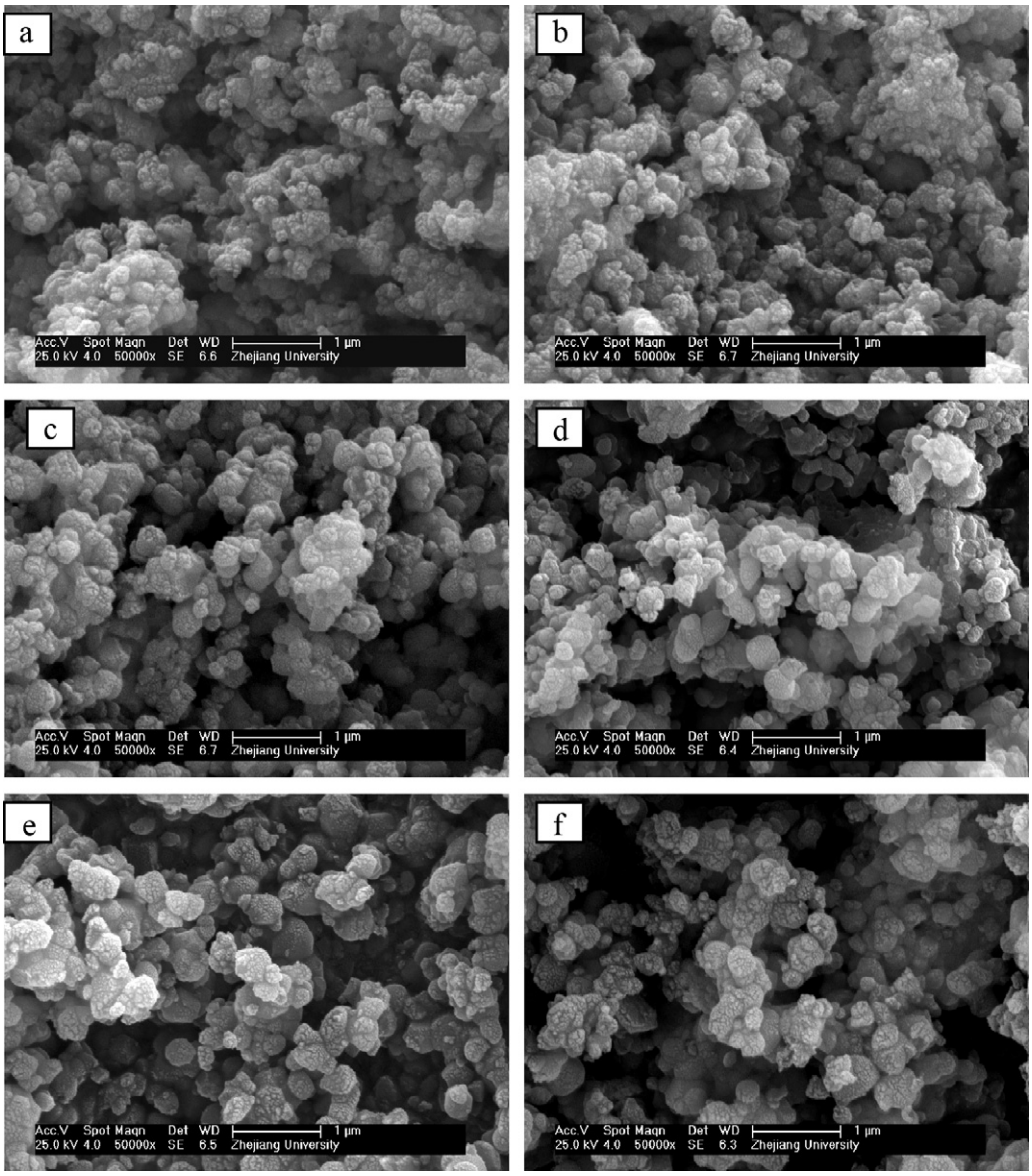

Fig. 1. SEM images of samples calcined at 700 °C in N_2 + 5 vol% H_2 atmosphere for different times: (a) 1 h, (b) 4 h, (c) 8 h, (d) 10 h, (e) 12 h, and (f) 14 h.

prepare carbon-free $LiFePO_4$ materials. Different calcination times were used in order to adjust the amount of Fe_2P/FeP. The structure and electrochemical performance of the materials prepared with different calcination times were analyzed, and an optimized amount of Fe_2P/FeP and the corresponding calcination time were suggested.

2. Experimental

Lithium carbonate, ferrous oxalate dihydrate and ammonium dihydrogen phosphate (chemicals purity >99%) were selected as starting materials in an amount based on the stoichiometric composition of $LiFePO_4$. The starting materials were ball milled for 3 h in acetone with a ball-to-powder weight ratio of 10:1 and a rotation speed of 300 rpm by using a planetary mill. The resulting suspension was pre-heated at 350 °C for 10 h in Ar, followed by another ball milling for 1 h in Ar. The ball milled intermediate product was then calcined at the temperature of 700 °C in N_2 + 5 vol% H_2 atmosphere for 1, 4, 8, 10, 12, and 14 h, respectively. These time series were designed so that the influence over the structure and performance of the synthesized $LiFePO_4$ composites can be investigated. A heating rate of 10 °C/min and a natural cooling in the furnace were adopted in the calcination process.

The morphology of the $LiFePO_4$ products was observed by scanning electron microscopy (SEM, Sirion-100, FEI). The particle size was measured using a particle size analyzer (LS13 320, Beckman coulter) after an ultrasonic dispersion in acetone. The phase structure of the products was analyzed by X-ray diffraction (X'Pert PRO, PANalytical) using Cu Kα radiation (λ = 1.54056 Å) by a step scanning method with a step interval of 0.02° and a count time of 1 s per step. The lattice parameters of the $LiFePO_4$, the phase composition and content of the products were analyzed by a Rietveld refinement method.

Electrochemical testing was carried out by coin cells of CR2025 with Li foil as anode and counter electrode and a microporous polyethylene sheet (Celgard 2400, Celgard) as separator. The cathodes were prepared by mixing the as-prepared $LiFePO_4$ product, acetylene black with polyvinylidene fluoride (PVDF) in a weight ratio of 75:15:10 in *N*-methyl-pyrolidinone, forming slurry, and subsequently pasting the slurry on an Al foil, followed by a heating at 120 °C for 14 h under vacuum. Then disks were punched from the foil in a diameter of 14 mm, followed a pressing of 6 MPa for 30 s. A typical cathode disk contained the $LiFePO_4$ product of about 3.6 mg/cm^2. A solution of 1 M $LiPF_6$ with ethylene carbonate (EC)/dimethyl carbonate (DMC) (1:1 by volume) was used as electrolyte. The cells were assembled in a glove box (Labstar, Braun) filled with high pure Ar.

The cells were galvanostatically cycled in a potential range of 2.0–4.3 V vs. Li/Li$^+$ at different discharge rates and the same charge rate of 0.1 C (1 C = 170 mA/g). The cells were activated for four cycles at charge and discharge rates of 0.1 C prior to the cycling at the different discharge rates, as it was found in the pre-study that there was a slight activation, i.e. the discharge capacity was slightly increased, in the first 3–4 cycles. Cyclic voltammetry (CV) tests were carried out using Arbin instruments (BT-2000, Arbin) in a voltage range of 2.5–4.3 V at a scan rate of 0.1 mV/s. Electrochemical impedance spectra (EIS) measurements were performed using a frequency response analyzer (Solartron 1255B, Solartron) equipped with an electrochemical interface (1287, Solartron) in a frequency range of 100 KHz to 0.01 Hz

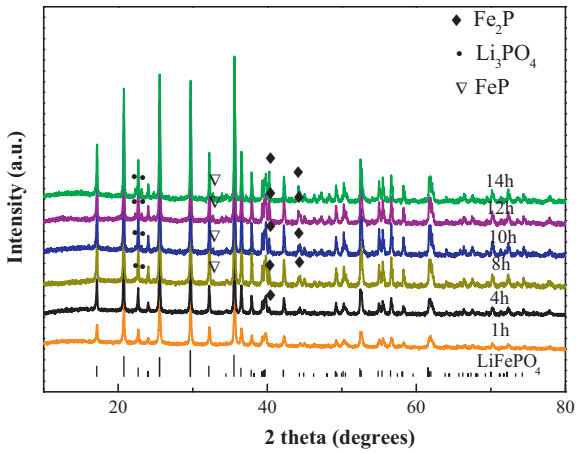

Fig. 2. XRD patterns of the $LiFePO_4$ products calcined at 700 °C in the atmosphere of N_2 + 5 vol% H_2 for different times.

and a potentiostatic signal amplitude of 5 mV was used. The cells used for EIS measurement were prepared in the same method used for the galvanostatical cycling as described above. The cells were also activated for 4 cycles at charge and discharge rates of 0.1 C between 2.5 and 4.3 V vs. Li/Li^+ prior to the EIS measurements, then polarized to 3.4 V and maintained the potential for 2 h. All of the electrochemical tests were performed at room temperature.

3. Results and discussion

3.1. Structure characterization

The morphologies of the $LiFePO_4$ products prepared by different calculation times are displayed in Fig. 1. As seen from Fig. 1, agglomeration exists in all the samples. But the agglomeration is severer for the products calcined for the shorter times of 1–4 h compared with those calcined for longer time. It is observed from Fig. 1 that the primary particles for the samples calcined for 1 and 4 h are smaller than that calcined for 8 h up to 14 h, as the agglomerated particles have no sufficient time to grow together in the short calcination times. However, the variation of the particle size of the samples is not obvious in the calcination time range of 8–14 h as seem from Fig. 1 (c)–(f)), indicating that the particle growth tend to be stable when the calcination time reaches 8 h.

The result of the particle size analysis by particle size analyzer showed that the mean diameter of the particles of the products increased gradually from 310 nm to 510 nm with the calcination time increasing from 1 h to 14 h. The measured values are very close to the primary size of the $LiFePO_4$ products, which are much smaller than the size of the agglomerates, especially for the samples calcined for short time of 1–4 h. As the samples were ultrasonic dispersed prior to the particle size measurement, the agglomerated particles, especially for the samples calcined for 1–4 h, should be partially de-agglomeration during ultrasonic dispersion process, and the measured particles were the dispersed ones, the size of which was close to the primary particles of the samples.

Fig. 2 displays the XRD patterns of samples calcined for different times. The Rietveld refinements results of the crystal structure and the phase composition are listed in Table 1. The largest value of the FWHM (full wave at half maximum) of the sample calcined for 1 h indicates its poorest crystallinity among all the samples. For the samples calcined for 4 h and longer, the values of FWHM tend to be smaller, indicating a better crystallization. Moreover, when the calcination time reaches 10 h and longer, the value of FWHM tends to be stable, indicating that the crystallinity tends to be stable. The lattice parameters almost do not change with the variation of the calcination time as seen from Table 1. However, the effect of the calcination time on the phase composition of the products is remarkable. XRD analyses (Fig. 2 and Table 1) show that only $LiFePO_4$ is detected for the sample calcined for 1 h. However, Fe_2P phase begins to arise when the calcination time is increased to 4 h. This implies that the formation of Fe_2P should after the formation of $LiFePO_4$. The content of Fe_2P/FeP increases gradually from 1.1 wt.% to 6.1 wt.% with the calcination time increasing from 4 to 14 h (Table 1). Moreover, minor FeP and Li_3PO_4 phases are also detected in the sample calcined for more than 8 h, and the content increases further with increasing calcination time. The formation of the Fe_2P/FeP and Li_3PO_4 is suggested from the reduction of $LiFePO_4$ [27]. In addition, from the analysis of the carbon content by the element analyzer (Flash EA 1112, ThermoFinnigan), the amount of carbon in the $LiFePO_4$ products calcined for different times is almost ignored, as no carbon source is used in the synthesis process.

3.2. Electrochemical characteristics

The charge–discharge curves of the samples calcined for different times at different discharge rates are shown in Fig. 3. The discharge specific capacity of the sample calcined for 1 h is the lowest for all discharge rates, which may be attributed mainly to the poor crystallinity as well as the sever agglomeration. Fig. 3(a) shows that the sample calcined for 4 h gives a most discharge specific capacity of 161 mAh/g in all of the samples at the discharge rate of 0.1 C, which reaches 95% of the theoretical capacity of $LiFePO_4$. This implies that the calcination time of 4 h has made $LiFePO_4$ well crystallized. Further seen from Fig. 3(b), the 4 h calcined sample still possesses the highest discharge capacity at the 1 C rate. In addition, as seen from Fig. 3(a) and (b), except for the sample calcined for 1 h, the discharge capacities of the samples at 0.1 C and 1 C rates decrease with the increase of the calcination time monotonously. But with the increase of the discharge rate, the order of the discharge capacity with the calcination time changes. As seen from Fig. 3(c)–(e), the samples calcined for 8 and 10 h tend to possess higher discharge capacity at the high discharge rates of 5–15 C. Thus, it is inferred that suitably increasing the calcination time is beneficial for the high-rate capability, but over prolongation of the calcination time (12–14 h) damages the high-rate capability on the

Table 1
The lattice parameters of $LiFePO_4$ and the phase composition of the samples calcined at 700 °C in N_2 + 5 vol% H_2 for different times obtained from Rietveld XRD refinement.

Calcination time (h)	Lattice parameter (Å)			FWHM (1 3 1) facet (°)	Phase content (wt.%)			
	a	*b*	*c*		$LiFePO_4$	Fe_2P	FeP	Li_3PO_4
1	10.322	6.006	4.694	0.20	100.0	–	–	–
4	10.324	6.007	4.694	0.15	98.9	1.1	–	–
8	10.322	6.006	4.693	0.14	94.3	2.7	1.2	1.8
10	10.322	6.006	4.693	0.13	91.2	3.7	1.4	3.6
12	10.322	6.006	4.694	0.13	88.6	4.4	2.3	4.6
14	10.322	6.006	4.693	0.13	84.3	6.1	3.5	6.1

Fitting satisfaction: $R_w/R_{exp} < 2$, R_w = 1.5–5.0%.

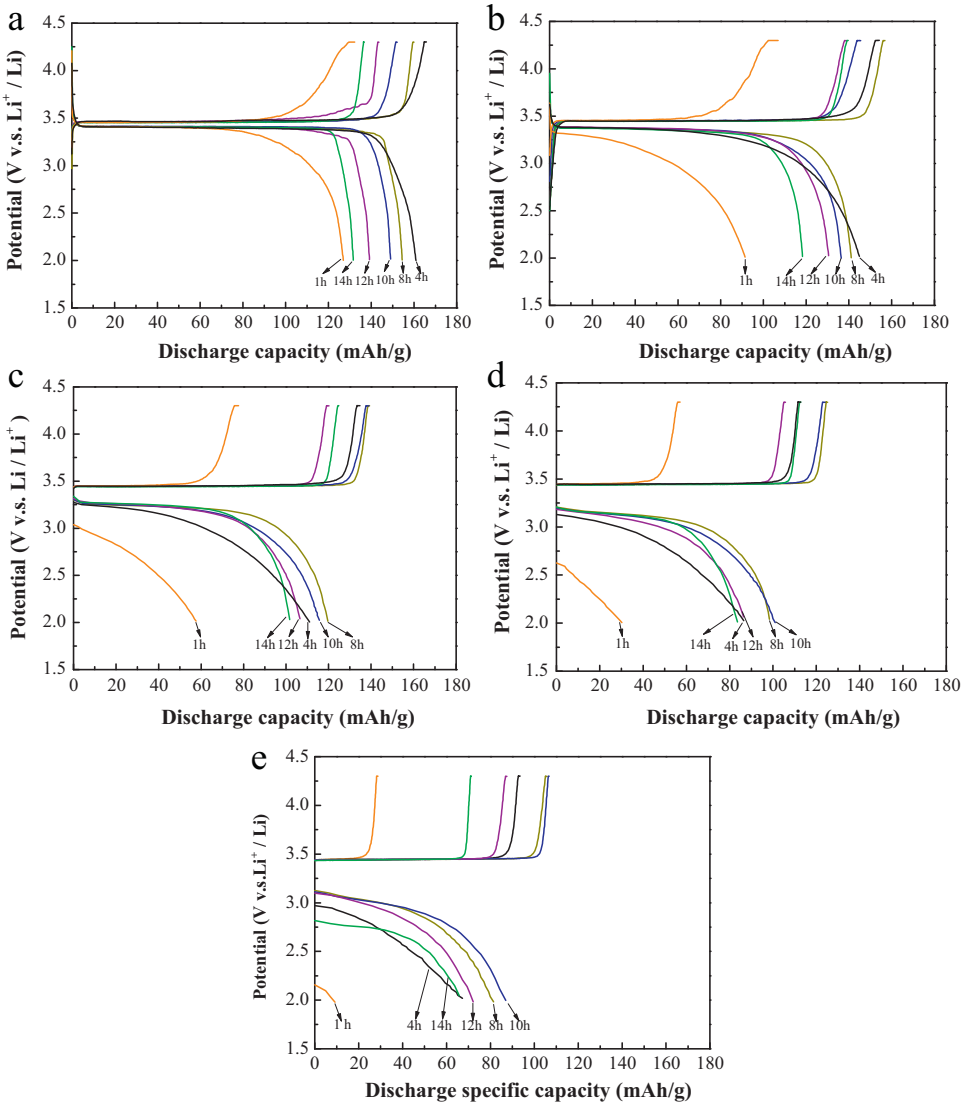

Fig. 3. The charge–discharge curve of the first cycle after the activation of the samples calcined for different times: (a) 0.1 C, (b) 1 C, (c) 5 C, (d) 10 C, and (e) 15 C.

contrary. Moreover, it is worth to note that the sample calcined for 4 h, which possesses the highest capacity at the low discharge rates of 0.1 C and 1 C, displays a larger decreasing tendency on the discharge capacity with the increase of the discharge rate compared with others, except for the one calcined for 1 h. At the discharge rate of 15 C, the sample calcined for 4 h shows almost the lowest discharge capacity among those samples calcined for 4–14 h (Fig. 3(e)).

Combining the structure and rate capability of the $LiFePO_4$ products calcined for different times, it is concluded that the existence of the high conductive phases of Fe_2P as well as FeP are important for the $LiFePO_4$ material obtaining favorable high-rate capability. Correlating the content of Fe_2P/FeP phases and the discharge capacity of the products at different discharge rates, it is evident that at lower discharge rates of 0.1 C and 1 C, the discharge capacity decreases with the increasing amount of Fe_2P/FeP in the case that the $LiFePO_4$ is in a similar well crystallinity. The main reason is suggested that at low discharge rate, the discharge capacity is not strongly affected by the electron conductivity, and the well crystallization and high fraction of $LiFePO_4$ are important for the extraction and insertion of more amount of lithium ions, which favors getting a high capacity. The higher amount of Fe_2P/FeP as well as the impurity of Li_3PO_4 lead to a low fraction of the active $LiFePO_4$ in the cathode, and hence result in a low specific capacity of the $LiFePO_4$ product.

However, the effect of the amount of Fe_2P/FeP on the discharge capacity at high discharge rates is different from it is at the low discharge rates. As seen from Fig. 3(c), when the discharge rate is increased to 5 C, the sample calcined for 8 h, which has a Fe_2P/FeP content of 3.9 wt.%, tends to possess the highest capacity, instead of the one calcined for 4 h, which has a lower content of Fe_2P. The sample calcined for 10 h, which has a much higher content of Fe_2P/FeP of 5.1 wt.%, states as the second, even the impurity of Li_3PO_4 is also much higher than the one calcined for 4 h. Moreover, at the higher discharge rates of 10 C and 15 C, the sample with suitably higher content of Fe_2P/FeP, prepared with a calcination temperature of 10 h, displays the largest capacity among all of the samples. Comparing the structure of the samples calcined for 4 h and 10 h, it is found that although the sample calcined for 10 h has slightly larger particle size for $LiFePO_4$ and higher amount impurity of Li_3PO_4, two factors of which are considered negative to the high-rate capability, the sample still shows better high-rate capability. This is contributed mainly to the suitably high amount of Fe_2P/FeP. Therefore, it is concluded that with the increase of the discharge rate, the role of Fe_2P/FeP in improving the high-rate capability becomes obvious. However, samples containing Fe_2P/FeP more than 6.7 wt.% and correspondingly Li_3PO_4 higher than 4.6 wt.%, which was obtained at calcination time of 12 and 14 h, do not show competitive capacity at discharge rates from 0.1 C to 15 C compared with those contain-

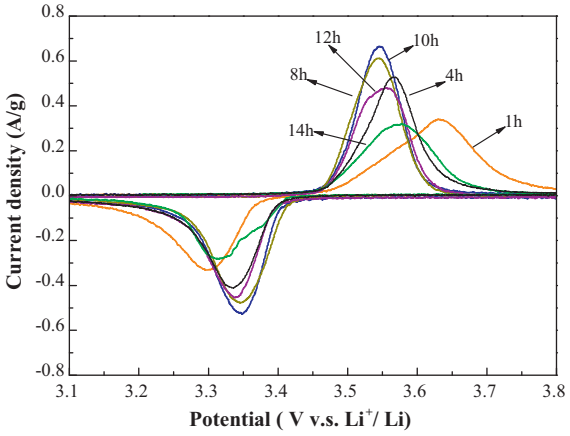

Fig. 4. CV profiles of the $LiFePO_4$ products calcined for different times.

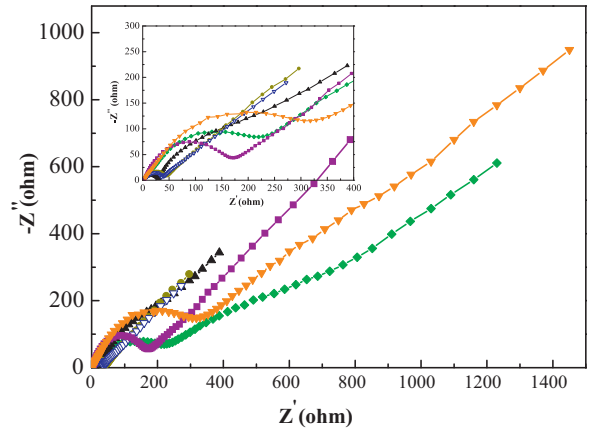

Fig. 5. EIS curves of the $LiFePO_4$ samples calcined for different times (▼, 1 h; ▲, 4 h; ●, 8 h; ▽, 10 h; ■, 12 h; and ♦, 14 h).

ing lower content of Fe_2P/FeP as well as Li_3PO_4, which was obtained at shorter calcination time, expect for the one calcined for 1 h. This indicates that the amount of Fe_2P/FeP needs to be carefully controlled, as they are inactive phase for the insertion and extraction of lithium ions and also cause the formation of impurity of Li_3PO_4. But the amount of Fe_2P as low as 1.1 wt.% (the sample calcined for 4 h) is not sufficient in improving high-rate capability. Therefore, it is believed that the $LiFePO_4$ material can provide desired high-rate capability when suitable amount of Fe_2P/FeP is introduced in situ, even the material almost without carbon coating and with particle size of submicron.

Fig. 4 is the CV profiles of the $LiFePO_4$ cathode with different calcination times. It is seen that the current density first increases and then decreases with the increase of the calcination time, reaching a maximum for the sample calcined for 10 h and that of the sample calcined for 8 h shows a close value as the second. The sharper and larger current density of the peak is, the better the reaction kinetics of the cathode is. Moreover, the potential difference between the anodic and cathodic peaks decreases firstly and then increases with the calcination time. The minimum value is obtained for the sample calcined for 10 h and then is the one calcined for 8 h. A smaller potential difference corresponds to a higher reversibility of lithiation and de-lithiation, thus a lower polarization. Hence, either the larger current density or the smaller potential difference of the samples calcined for 8 and 10 h indicates that they provide the most favorable reaction kinetics compared with the others. The result from the CV measurement is in good agreement with the discharge capacity at the high discharge rates. Suitable amount of Fe_2P/FeP increases the electron conductivity of the $LiFePO_4$ product, therefore, improves the reaction kinetics of the lithiation and de-lithiation during cycling. It was ever reported that Fe_2P formed as inclusion at the surface of $LiFePO_4$ particles [28]. Such a $LiFePO_4$/iron phosphides composite material consists of conductive surface covered with iron phosphides, which plays a role of conductive paths within the whole sample [19]. Such conductive paths contribute the kinetics of Li ion transfer. However, as reported by Islam et al. [29], the excessive introduction of Fe_2P to the $LiFePO_4$ material would disrupt the one-dimension pathway for lithium ion transportation within the particle, and consequently hinder the Li^+ diffusion. Samples calcined for 12 h and longer which contain excess content of Fe_2P/FeP as well as impurity Li_3PO_4 show worsening reaction kinetics compared the sample calcined for 10 or 8 h.

The electrochemical impedance curves of the $LiFePO_4$ cathode with different calcination times are illustrated in Fig. 5. The inset is the amplification of the high frequency region. The intercept of the curve at high frequency to the real axis relates to the bulk resistance of electrolyte (R_e). The two depressed semicircles in the medium-high and medium-low frequency regions relate to the resistance from the solid-electrolyte interface film formed on the surface of the cathode due to the reaction with the electrolyte (R_{film}) and the charge transfer resistance (R_{ct}) at the particle surfaces, respectively [30]. The straight line in the low frequency region, namely the Warburg resistance Z_w, is attributed to the diffusion resistance of lithium ions within the $LiFePO_4$ particles. The impedance spectra can be described by the following equivalent circuit [31]:

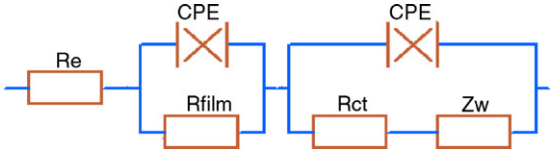

where CPE (the constant phase elements) denotes the double layer capacitance. By using the Zplot® software, the charge-transfer resistances of the products are obtained and listed in Table 2. Besides, the diffusion coefficients of lithium ions within the particle of the $LiFePO_4$ products are calculated by the following equations [32,33] and are also listed in the Table 2.

$$Z_{re} = R_e + R_{film} + R_{ct} + \sigma\omega^{-0.5}$$

$$D = \frac{R^2T^2}{2A^2n^4F^4c^2\sigma^2}$$

Herein, σ is the Warburg coefficient, ω is the angular frequency in the low frequency region, R is the gas constant, T is the absolute temperature, A is the surface area of the cathode, n is the number of

Table 2
The charge transfer resistance (R_{ct}) and the diffusion coefficient (D) of Li-ion of the $LiFePO_4$ products calcined for different times.

	Calcination time (h)					
	1	4	8	10	12	14
R_{ct} (Ω)	273.5	219	42.21	39.9	180.4	234.7
D (cm^2/s)	7.63×10^{-15}	5.82×10^{-14}	6.80×10^{-14}	8.15×10^{-14}	1.14×10^{-14}	6.21×10^{-15}

electrons per molecule during oxidization, F is the Faraday constant, and c is the concentration of lithium ions.

Table 2 shows that with the calcination time increasing from 1 h to 10 h, the charge transfer resistance decreases and the diffusion coefficient of lithium ions increases, despite that there is a slight increase of the $LiFePO_4$ particles, which commonly increases the charge transfer resistance and decreases the diffusion coefficient. The improvement of the rates charge transfer and the diffusion of lithium ions with the calcination temperature from 1 h to 10 h is inferred due to the suitably increasing of the Fe_2P/FeP content which increases the electron conductivity of the $LiFePO_4$ material and the improvement of the crystallinity of the $LiFePO_4$ phase. The low charge transfer resistance and the high diffusion coefficient of lithium ions for the sample calcined for 10 h as well as 8 h indicate that the high reaction kinetics of the samples is consistent highly with their high-rate capability. However, the further increase of calcination time deteriorates either the charge transfer or the diffusion of lithium ions, which is due partially to the formation of higher content of impurity of Li_3PO_4. Besides, the excess amount of Fe_2P/FeP should also act as barriers for the lithium ion diffusion, which in turn increases the resistance associated with the charge transfer process.

4. Conclusions

Carbon-free $LiFePO_4$ materials with a few amounts of Fe_2P/FeP phases were synthesized by a mechanical activation method. The formation of Fe_2P/FeP is calcination time dependent. By calcined at 700 °C for 1–14 h at the atmosphere of N_2 + 5 vol% H_2, the amount of Fe_2P/FeP phases varies from 1 to 10 wt.%. Impurity of Li_3PO_4 forms with the formation of Fe_2P/FeP. The existence of Fe_2P/FeP is found less important for the discharge capacity at low discharge rates of 0.1 C and 1 C. The $LiFePO_4$ material containing trace Fe_2P shows higher discharge capacity at low discharge rate than those containing higher Fe_2P/FeP phases. But suitably higher content of Fe_2P/FeP plays important role in improving the high-rate capability of the $LiFePO_4$ material. 4–5 wt.% Fe_2P/FeP is favorable for $LiFePO_4$ materials getting high capacity at discharge rate higher than 5 C, in which case discharge capacities of 116, 101 and 87 mAh/g are obtained at rates of 5 C, 10 C and 15 C, respectively. Suitable amount of Fe_2P/FeP decreases charge transfer resistance and increases the diffusion coefficient of lithium ions, hence favoring the high-rate capability. But excess amount of Fe_2P/FeP and the accordingly high amount of Li_3PO_4 lower the fraction of $LiFePO_4$ in the cathode and also deteriorate the reaction, resulting in a low rate capacity of the cathode.

Acknowledgements

The work was supported by National Natural Science Foundation for Distinguished Young Scholars of P. R. China (No. 51025102), and by National Natural Science Foundation of P. R. China (No. 50871100).

References

[1] A.K. Padhi, K.S. Nanjundaswamy, J.B. Goodenough, J. Electrochem. Soc. 144 (1997) 1188–1194.
[2] K. Striebel, J. Shim, V. Srinivasan, J. Newman, J. Electrochem. Soc. 152 (2005) A664–A670.
[3] P.P. Prosini, M. Lisi, D. Zane, M. Pasquali, Solid State Ionics 148 (2002) 45–51.
[4] A. Dell'Era, M. Pasquali, J. Solid State Electrochem. 13 (2009) 849–859.
[5] B. Zhao, Y. Jiang, H.J. Zhang, H.H. Tao, M.Y. Zhong, Z. Jiao, J. Power Sources 189 (2009) 462–466.
[6] J.K. Kim, G.S. Chauhan, J.H. Ahn, H.J. Ahn, J. Power Sources 189 (2009) 391–396.
[7] H. Liu, J.Y. Xie, K. Wang, J. Alloys Compd. 459 (2008) 521–525.
[8] X.K. Zhi, G.C. Liang, L. Wang, X.Q. Ou, L.M. Gao, X.F. Jie, J. Alloys Compd. 503 (2010) 370–374.
[9] J. Ni, M. Morishita, Y. Kawabe, M. Watada, N. Takeichi, T. Sakai, J. Power Sources 195 (2010) 2877–2882.
[10] M. Konarova, I. Taniguchi, J. Power Sources 195 (2010) 3661–3667.
[11] S.Y. Chung, J.T. Bloking, Y.M. Chiang, Nat. Mater. 1 (2002) 123–128.
[12] X. Yin, K. Huang, S. Liu, H. Wang, H. Wang, J. Power Sources 195 (2010) 4308–4312.
[13] X.J. Chen, G.S. Cao, X.B. Zhao, J.P. Tu, T.J. Zhu, J. Alloys Compd. 463 (2008) 385–389.
[14] L.J. Li, X.H. Li, Z.X. Wang, H.J. Guo, L. Wu, Y. Hao, et al., J. Alloys Compd. 497 (2010) 176–181.
[15] C.F. Li, N. Hua, C.Y. Wang, X.Y. Kang, T. Wumair, Y. Han, J. Alloys Compd. 509 (2011) 1897–1900.
[16] H.J. Kim, J.M. Kim, W.S. Kim, H.J. Koo, D.S. Bae, H.S. Kim, J. Alloys Compd. 509 (2011) 5662–5666.
[17] C.G. Son, H.M. Yang, G.W. Lee, A.R. Cho, V. Aravindan, H.S. Kim, et al., J. Alloys Compd. 509 (2011) 1279–1284.
[18] P.S. Herle, B. Ellis, N. Coombs, L.F. Nazar, Nat. Mater. 3 (2004) 147–152.
[19] J. Molenda, J. Marzec, Funct. Mater. Lett. 1 (2008) 97–104.
[20] Y. Lin, M.X. Gao, D. Zhu, Y.F. Liu, H.G. Pan, J. Power Sources 184 (2008) 444–448.
[21] M.S. Song, D.Y. Kim, Y.M. Kang, Y.I. Kim, J.Y. Lee, H.S. Kwon, J. Power Sources 180 (2008) 546–552.
[22] Y. Kadoma, J.M. Kim, K. Abiko, K. Ohtsuki, K. Ui, N. Kumagai, Electrochim. Acta 55 (2010) 1034–1041.
[23] Z.H. Chen, J.R. Dahn, J. Electrochem. Soc. 149 (2002) A1184–A1189.
[24] D.H. Kim, J. Kim, Electrochem. Solid State Lett. 9 (2006) A439–A442.
[25] C.R. Sides, F. Croce, V.Y. Young, C.R. Martin, B. Scrosati, Electrochem. Solid State Lett. 8 (2005) A484–A487.
[26] T. Nakamura, Y. Shima, H. Matsui, Y. Yamada, S. Hashimoto, H. Miyauchi, et al., J. Electrochem. Soc. 157 (2010) A544–A549.
[27] Y.-H. Rho, L.F. Nazar, L. Perry, D. Ryan, J. Electrochem. Soc. 154 (2007) A283–A289.
[28] W. Ojczyk, J. Marzec, K. Swierczek, W. Zajac, M. Molenda, R. Dziembaj, et al., J. Power Sources 173 (2007) 700–706.
[29] M.S. Islam, D.J. Driscoll, C.A.J. Fisher, P.R. Slater, Chem. Mater. 17 (2005) 5085–5092.
[30] J. Morales, R. Trocoli, E. Rodriguez-Castellon, S. Franger, J. Santos-Pena, J. Electroanal. Chem. 631 (2009) 29–35.
[31] C. Ho, I.D. Raistrick, R.A. Huggins, J. Electrochem. Soc. 127 (1980) 343–350.
[32] B. Jin, E.M. Jin, K.H. Park, H.B. Gu, Electrochem. Commun. 10 (2008) 1537–1540.
[33] A.Y. Shenouda, H.K. Liu, J. Alloys Compd. 477 (2009) 498–503.